Solar Energy Materials & Solar Cells 98 (2012) 300–307

Contents lists available at SciVerse ScienceDirect

Solar Energy Materials & Solar Cells

journal homepage: www.elsevier.com/locate/solmat

Influence of molecular weight on silole-containing cyclopentadithiophene polymer and its impact on the electrochromic properties

Jen-Hsien Huang [a], Annie Tzuyu Huang [a], Chih-Yu Hsu [b], Jiann-Tsuen Lin [b], Chih-Wei Chu [a,c,*]

[a] Research Center for Applied Sciences, Academia Sinica, Taipei 11529, Taiwan
[b] Institute of Chemistry, Academia Sinica, Taipei 11529, Taiwan
[c] Department of Photonics, National Chao-Tung University, Hsinchu 30010, Taiwan

ARTICLE INFO

Article history:
Received 7 July 2011
Received in revised form
2 November 2011
Accepted 11 November 2011
Available online 3 December 2011

Keywords:
Electrochromic
Polymer
Molecular weight
Electrochemistry
Mobility

ABSTRACT

In this article, we have systematically studied the effect of molecular weight on poly[(4,4′-bis(2-ethylhexyl)dithieno[3,2-b:2′,3′-d]silole)-2,6-diyl-*alt*-(5,5′-thienyl-4,4′-dihexyl-2,2′bithiazole)-2,6-diyl], a novel cathodically coloring electrochromic polymer. The polymer with higher molecular weight can stack much better due to the stronger π–π^* interaction and was found to exhibit better charge transfer property and lower internal resistance. These results have shown to enhance the coloration efficiency of the polymer remarkably. For the molecular weight of 33.6 kg/mol, the coloration efficiency is 423 cm^2/C, much higher compared with the low molecular weight polymer (6.3 kg/mol, 226 cm^2/C).

© 2011 Elsevier B.V. All rights reserved.

1. Introduction

Conjugated polymers have received much attention throughout the course of the past two decades, stemming not only from their high conductivity in the doped state but also from a variety of optoelectronic and redox properties. One of these properties is electrochromism defined as a reversible optical absorbance/transmittance change in response to an externally applied potential. Compared with inorganic materials, conjugated polymers possess many superior properties over the counter part, including rapid response times, larger contrast, lower power requirements, multicolor, higher coloration efficiency (CE) and the capability to structurally modify the chemical structure to achieve specific color or function [1–6].

Among these properties, CE is the most important parameter for electrochromic materials defined by the relationship between the injected/ejected charge, electrode area and the change in optical density (ΔOD) at a specific wavelength. An ideal or high CE electrochromic material should exhibit a large transmittance change (Δ%T) with a small injected/ejected charge. Recently, CE of conjugated polymers can be enhanced by blending carbon nanotubes or other conducting materials into the polymer matrix. The resulting conductive network can lead to lower internal resistance and give rise to larger CE [7–10]. Alternatively, the improvement of CE can also be achieved through fabrication engineering, i.e. by controlling the growth rate of polymer films that can increase the degree of packing for polymer chains. Consequently, the unique stacking properties of conjugated polymers can result in higher charge mobility and reduced resistance thus leading to high CEs [11]. Besides these methods, another influenced factor comes from the regioregularity of the polymer chains. Jain et al. have reported that the regioregular water-soluble conjugated polymer exhibits better CE compared with the corresponding water-soluble regiorandom polymers [12]. Intrinsically, the mechanism for the enhancement of CE is very similar either by controlling the film growth rate or the regioregularity of the polymer chains. These two methods both enhance the polymer chain packing and therefore better optoelectronic properties by forming stronger chain interactions. This indicates that the interaction between polymer chains is critical and it is important to explore the effect of molecular weight (MW) on the polymer based electrochromic properties.

Recent studies have shown that the variation of polymer MW can cause significant impact on the optoelectronic device performance. Kline et al. have concluded that poly(3-hexylthiophene) (P3HT) based field effect transistor with higher MW have higher mobility because the regions of crystalline order are less well defined [13]. The morphology and performance of bulk heterojunction solar cells comprised of polythiophene and polyfluorene

* Corresponding author at: Research Center for Applied Sciences, Academia Sinica, Taipei 11529, Taiwan.
E-mail address: gchu@gate.sinica.edu.tw (C.-W. Chu).

0927-0248/$ - see front matter © 2011 Elsevier B.V. All rights reserved.
doi:10.1016/j.solmat.2011.11.019

based polymer have been investigated with different MWs. It was concluded that devices made of higher MW polymer exhibit higher performance because of the longer conjugation length of the polymer chain and better interconnections within the bicontinuous network [14–16]. Hosoi et al. [17] also fabricated polymeric light-emitting diodes using poly(9,9-dioctylfluorene) (PDOF) with different MWs. They found that electroluminescence characteristics of devices using the PDOF with the high MW component were superior to those of the devices using PDOF with the low MW component [17]. However, the effect of MW on electrochromic properties is still not clear. It has been shown that, at similar thicknesses, the cyclopentadithiophene (CPDT)-based polymers have higher optical density change and CE compared to PEDOT and its derivatives [18,19]. It will be interesting to know the correlation between the MW and electrochromic properties. Here, we synthesized poly[(4,4′-bis(2-ethylhexyl)dithieno[3,2-b:2′,3′-d]silole)-2,6-diyl-*alt*-(5,5′-thienyl-4,4′-dihexyl-2,2′-bithiazole)-2,6-diyl] (Si-PCPDTTBT) with various MWs to investigate the impact of MW on its electrochromic properties.

2. Experimental

2.1. Synthesis

Monomers M1 and M2 were synthesized according to a reported procedure [20,21], and the characterization is described as follows. The synthetic route of copolymer Si-PCPDTTBT is shown in Scheme 1, and the procedure is described as follows:

M1. Yield: 65%. ^{1}H NMR: δ 7.03 (d, 2H), 6.92 (d, 2H), 2.86 (t, 4H), 1.72 (m, 4H), 1.40–1.15 (m, 12H), 0.86 (t, 6H). EI-MS: *m*/*z* 656. M2. Yield: 92%. ^{1}H NMR: δ 7.06 (s, 2H), 1.68 (m, 2H), 1.4–1.13 (m, 16H), 0.90 (t, 6H), 0.83 (t, 6H), 0.74 (m, 4H), 0.32 (s, 18H).

A solution of M1 (2.00 g, 2.68 mmol) and M2 (1.70 g, 2.68 mmol) in toluene (40 mL) was purged with Ar for 10 min and then $Pd(PPh_3)_4$ (0.150 g, 0.134 mmol) and triphenylphosphine (0.21 g, 0.80 mmol) were added. After purging with Ar for 20 min, the mixture was heated under reflux for 48 h in an oil bath set at 110 °C under an Ar atmosphere. The mixture was cooled to room temperature, MeOH (100 mL) was added, and the precipitated polymer was filtered out. After Soxhlet extraction with MeOH, hexane and $CHCl_3$, the polymer was recovered from the $CHCl_3$ phase through reprecipitation with MeOH and then dried under vacuum for 1 day (40%). The MW of polymer was controlled by changing the reaction time, which was monitored by GPC. In this study, Si-PCPDTTBT with four different MWs was synthesized. The reaction times were 6, 10, 24 and 48 h respectively. The detail information of the MWs for the as-prepared polymers are shown in Table 1.

2.2. Polymer thin-film deposition

Prior to deposition, Si-PCPDTTBT was dissolved in 1,2,-dichlorobenzene and then stirred for 12 h at 50 °C. Before polymer deposition, the ITO glasses (2×2 cm^2) were ultrasonically cleaned in detergent, de-ionized water, acetone and isopropyl alcohol before the deposition. After routine solvent cleaning, the substrates were treated with UV ozone for 15 min. Consequently, the polymer films were deposited through spin coating with a spin rate of 2000 rpm.

2.3. Characterization

Thermal gravimetric analysis (TGA) was conducted to characterize the thermal stability of Si-PCPDTTBT powder using DuPont 951 from room temperature to 850 °C with a heating rate of 10 °C min^{-1} in nitrogen atmosphere. Spectroelectrochemical data were recorded using a Shimadzu UV-1601PC spectrophotometer. Surface morphologies of thin films were obtained using atomic force microscopy (AFM, Digital instrument NS 3a controller with D3100 stage). X-ray diffraction (XRD) analyses were performed using a Philips X'Pert/MPD instrument. For EIS analysis, the P3HT electrodes were

Table 1
Summary of the MWs, polydispersities (PDI) and yields of Si-PCPDTTBT samples in this study.

Sample of Si-PCPDTTBT	M_n[a] (kg/mol)	M_w[a] (kg/mol)	PDI	Yield (%)
Low MW	6.3	12.2	1.93	61
Medium MW	12.7	15.7	1.23	55
	22.9	27.3	1.19	57
High MW	33.6	38.9	1.15	56

[a] Molecular weights and polydispersity were measured by GPC, using THF as an eluent, polystyrene as a standard. M_n—number average molecular weight. M_w—weight average molecular weight.

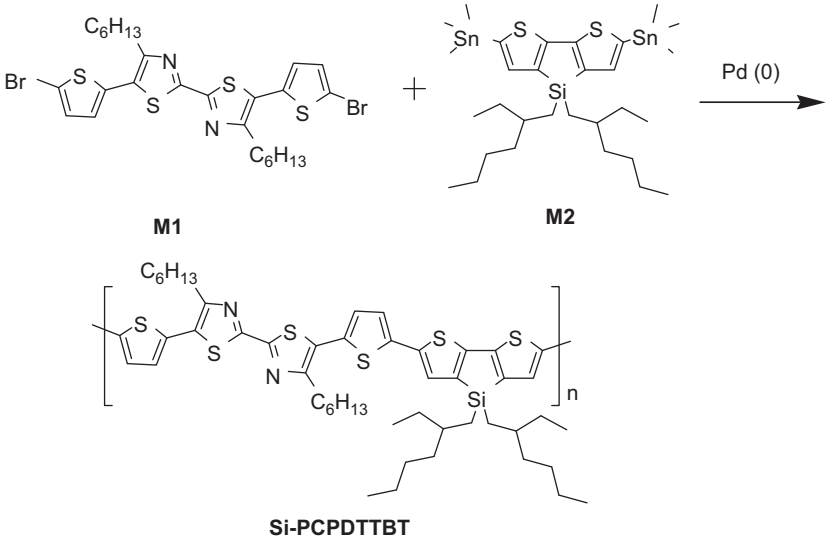

Scheme 1. Synthetic route of Si-PCPDTTBT copolymer.

characterized using a three-electrode system (the potentiostat mentioned above) equipped with an FRA2 module in the presence of 1.0 mM redox couples and 0.1 M $LiClO_4$ in aqueous solution. The impedance spectra were recorded at the formal potential of the redox couple in the frequency ranging from 100 to 10,000 Hz. The impedance spectra were fitted to an equivalent circuit model proposed by Sundfors et al. [22] and the model parameters were obtained using ZView software. Colorimetry measurements were performed using a Minolta CS-100 Chroma Meter; the sample was illuminated from behind using a D50 (5000 K) light source. A background measurement was taken from blank ITO in an electrolyte solution held in a standard quartz cuvette.

3. Results and discussion

Table 1 summarizes the MWs, polydispersities (PDI) and yield of the Si-PCPDTTBT samples used in this study. It should be mentioned that the solubility of Si-PCPDTTBT becomes very poor with MW larger than 33.6 kg/mol (M_n). From Table 1, it can be found that increasing Si-PCPDTTBT MW also leads to lower PDI. In general, polymer with larger PDI would results in amorphous structure. This is due to the polymer chains disruption contributed from the smaller polymer segment. However, for large MW polymer, the narrow PDI can enhance the crystallinity due to the better polymer chain packing [23]. TGA thermograms recorded under nitrogen atmosphere for the Si-PCPDTTBT with various MWs are shown in Fig. 1. A drastic weight loss was observed in the temperature range of 400–500 °C for the Si-PCPDTTBT followed by a continuous gradual weight loss. In addition, the onset temperature of 10% weight loss for the polymer is found to increase with increasing MW. The decreasing thermal stability with the decreasing molecular weight is expected as it has been observed in many polymer systems.

The absorption spectra of the Si-PCPDTTBT films with different MWs are shown in Fig. 2. The absorption peaks show a trace of red shift in Si-PCPDTTBT thin film. The corresponding images for the polymer solution with various MWs are shown in the inset of Fig. 2. The conjugation length of the polymer increases with its

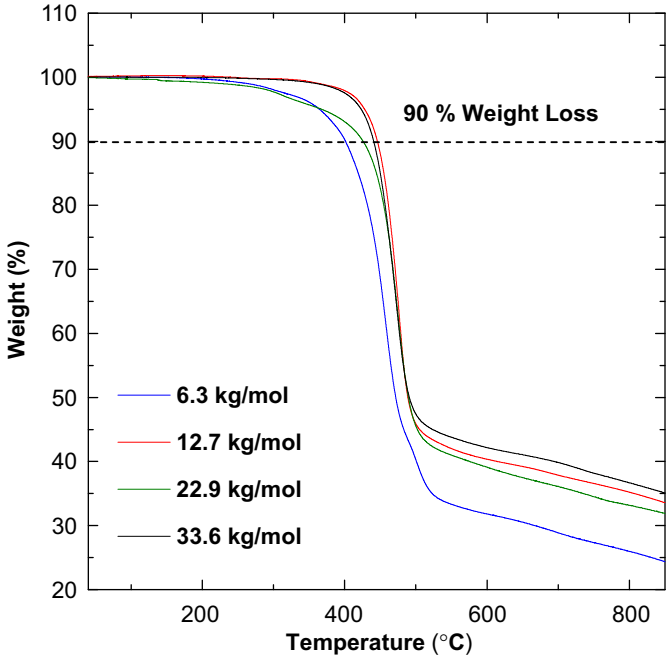

Fig. 1. Thermal stability of Si-PCPDTTBT with various MWs.

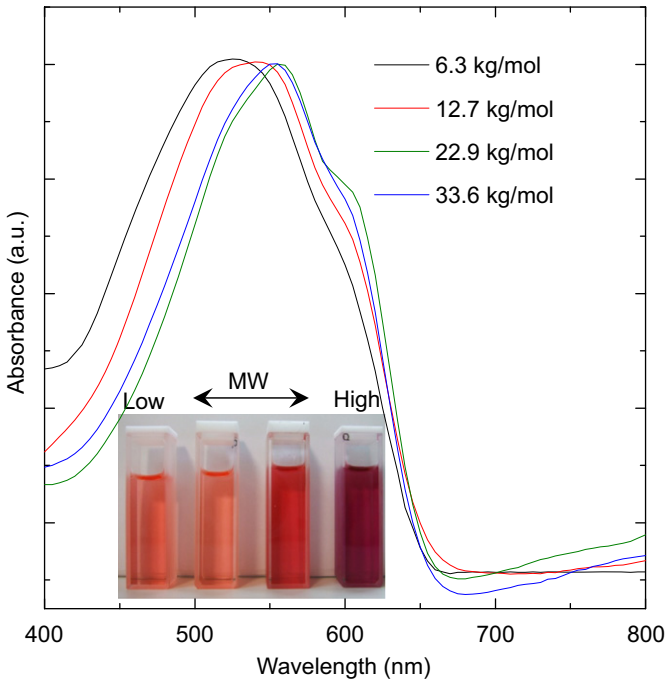

Fig. 2. Optical absorption of Si-PCPDTTBT with various MWs. The red-shift of the absorption indicates the larger orbital delocalization by virtue of longer conjugated polymer chains (inset: the corresponding solution images). (For interpretation of the references to color in this figure legend, the reader is referred to the web version of this article.)

MW. Therefore, the extent of red shift in the absorption spectrum increases with its MW as well. Moreover, the vibronic peak appeared in the high MW Si-PCPDTTBT film indicated the formation of π–π stacking resulting in an ordered structure. The conformation of ordered structured facilitates the delocalization of π-electrons and an increase in conjugation length that results in a red shift of absorption spectrum.

Fig. 3 presents the optoelectrochemical spectral series obtained from Si-PCPDTTBT films with different MWs while changing from the reduced state to the fully oxidized state. In the neutral state, the polymer showed a λ_{max} of 520 nm because of the π–π^* transition. An optical band gap of 1.82 eV was calculated from the onset of the π–π^* transition. Upon stepwise oxidation, the reduction in absorption due to the decrease in π–π^* transition results in a very transmissive polymer film which indicates that the Si-PCPDTTBT is a cathodically coloring material. The polymer shows a well-defined isosbestic point at around 620 nm, which implies that only one kind of chromophoric species is involved. Moreover, we found that the Si-PCPDTTBT with higher MW exhibits larger optical contrast between darkened and bleached states. The ΔODs of the Si-PCPDTTBT films obtained between 0.0 and 1.0 V are 0.23, 0.33, 0.37 and 0.42 for the MW of 6.3, 12.7, 22.9 and 33.6 kg/mol, respectively.

The surface morphology of the Si-PCPDTTBT films was characterized by AFM as shown in Fig. 4. The morphologies of Si-PCPDTTBT films are distinctly different while varying the MWs. At low MW, the sample exhibits smooth surface topography with featureless morphology. With the increasing of the MWs, the surface morphologies become more and more uneven which may be originated from the enhancement of interchain stacking. The polymer films with 6.3 kg/mol, 12.7 kg/mol, 22.9 kg/mol and 33.6 kg/mol MW exhibit a root-mean-square surface roughness of 1.3 nm, 1.6 nm, 2.1 nm and 2.7 nm, respectively. The images suggest that the higher MW samples are more crystalline.

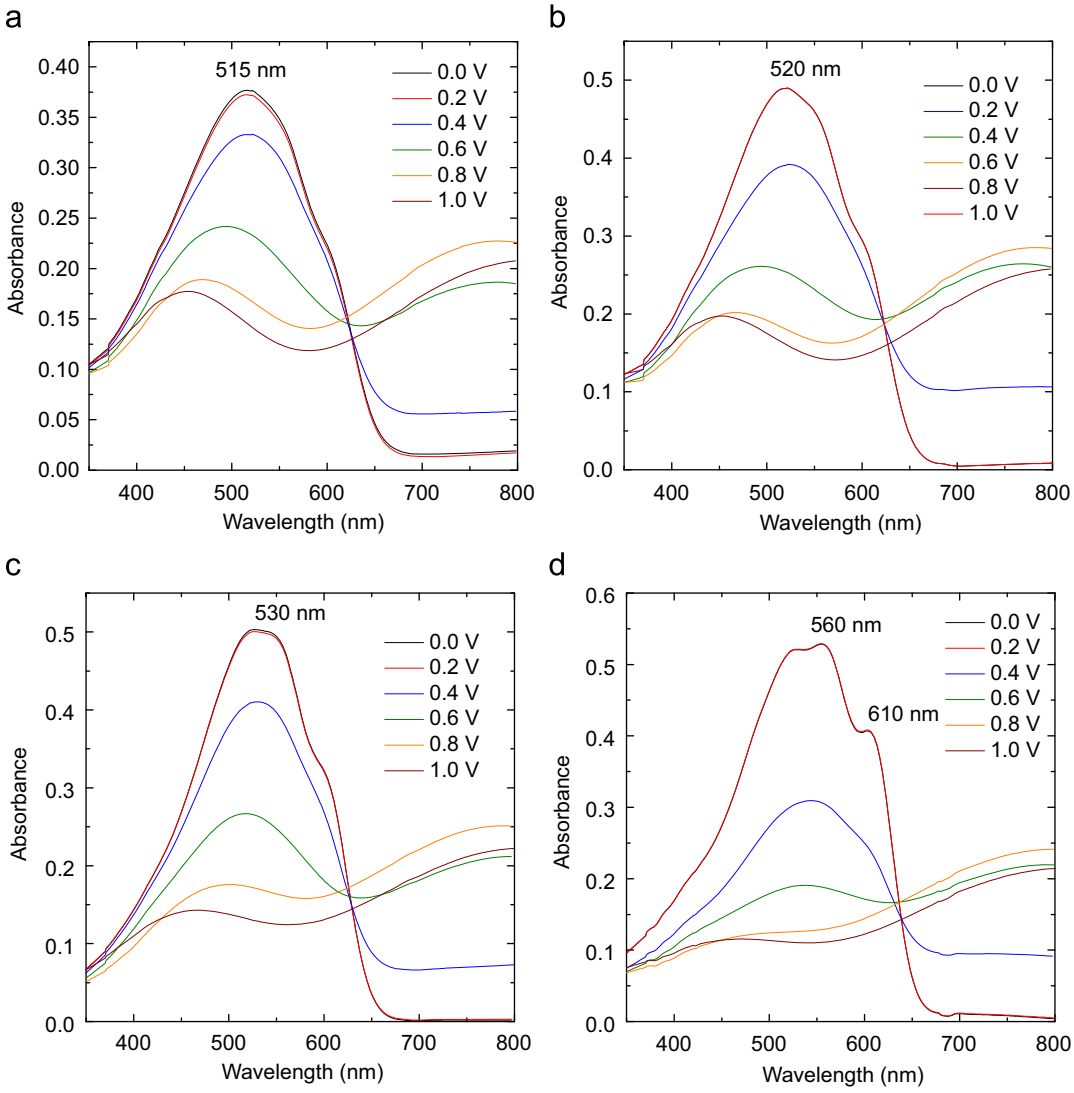

Fig. 3. *In situ* UV–vis absorption spectra of films of the Si-PCPDTTBT with various MWs at various potentials (0.0–1.0 V vs. Ag/Ag^{+}) in 0.1 M $LiClO_4$/acetonitrile: (a) 6.3 kg/mol, (b) 12.7 kg/mol, (c) 22.9 kg/mol and (d) 33.6 kg/mol.

To further investigate the crystallinity of the polymer films, XRD was used to study the property of polymer films. As shown in Fig. 5a, the low MW Si-PCPDTTBT exhibits an amorphous pattern indicating the disordered structure. Increased intensity is observed with increasing MW in the peak at $2\theta = 6.17^{\circ}$, which corresponds to the layering distance, $d_{100} = 14.3$ Å, between the sheets of Si-PCPDTTBT chains associated with the plane perpendicular to their longitudinal axes. The increase of crystallinity can enhance charge transfer within the polymer films because of the reduction of charge transfer barrier [15,24–28]. This can be confirmed by the measurement of charge mobility as shown in Fig. 4b. Here, we measure the hole mobility of Si-PCPDTTBT by fabricating the hole only devices. The structure of hole only device is shown in the inset of Fig. 5b. To block the electron current, the polymer films were spin coated on the poly(ethylenedioxythiophene):polystyrenesulfonate modified ITO substrate and capped with V_2O_5/Al. The curves were fitted with space-charge limited current model to calculate charge mobility. The calculation used was $J = 9\varepsilon_0\varepsilon_r\mu V^2/8L^3$ [29], where $\varepsilon_0\varepsilon_r$ is the permittivity of the polymer, μ is the carrier mobility and L is the device thickness. With the increasing of the MW, the calculated charge mobilities of Si-PCPDTTBT are 7.2×10^{-8}, 8.3×10^{-8}, 1.0×10^{-7} and 1.2×10^{-7} m^2/V s, respectively. The higher mobility of Si-PCPDTTBT is attributed from the stronger crystallinity and more favorable morphology.

To investigate the kinetics of the electron transfer at the polymer–solution interface, we characterized the polymer films using electrochemical impedance spectroscopy (EIS). Fig. 6 displays the impedance spectra of the polymer films characterized under 1.0 mM $K_4Fe(CN)_6$, $K_3Fe(CN)_6$ and 0.1 M $LiClO_4$ as the supporting electrolyte. We fitted the EIS data with the equivalent circuit [22] presented in the inset of Fig. 6. In the equivalent circuit, R_s is the solution resistance, R_{ct} is the charge transfer resistance due to electron transfer at the polymer–solution interface, Z_w is the infinite-length Warburg diffusion impedance due to diffusion of the redox couple in the solution, C_d is the electronic capacitance of the polymer film and Z_d is the finite-length Warburg diffusion impedance due to diffusion of charge compensating counterions in the polymer film. The fitting results are presented in Fig. 6, where the solid lines represent the modeling results obtained by fitting the dotted experimental data. The fitted results suggest that the values of R_{ct} of the Si-PCPDTTBT are 1203, 957, 894 and 427 Ω for the increasing of the MW from 6.3 to 33.6 kg/mol. The small value of R_{ct} of the high MW film was resulted from its highly ordered structure, which provided a larger charge mobility, leading to a lower resistance at the

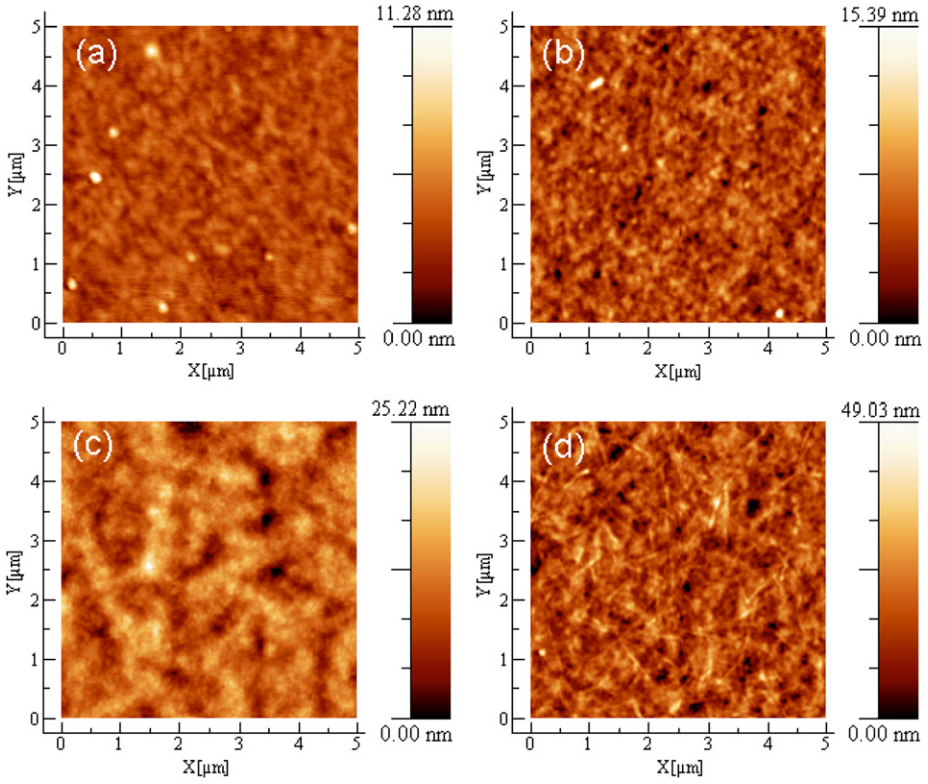

Fig. 4. The AFM images of Si-PCPDTTBT films with various MWs: (a) 6.3 kg/mol, (b) 12.7 kg/mol, (c) 22.9 kg/mol and (d) 33.6 kg/mol.

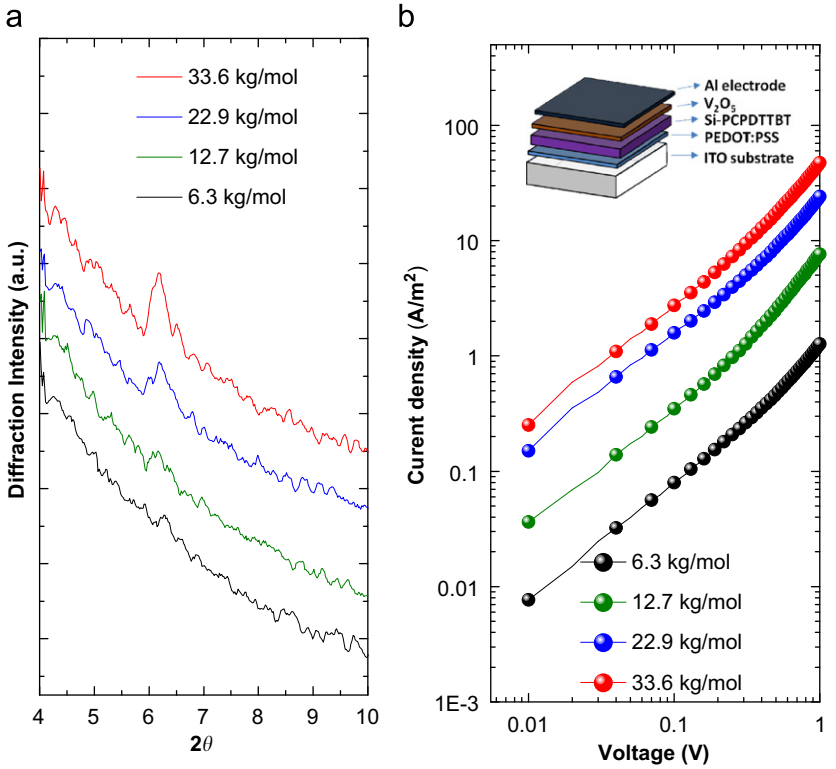

Fig. 5. The XRD pattern of the Si-PCPDTTBT thin films with various MWs and the corresponding *J–V* curves for hole only devices.

polymer–electrolyte interface. We obtained the rate constant of the electron transfer (k_0) using $k^0=((RT)/(n^2F^2R_{ct}AC))$ [22], where A is the area of the electrode, C is the bulk concentration of the redox couple and other symbols have their usual electrochemical meanings. Using the known values of R_{ct}, we calculated the values of k_0 for the polymer films to be 2.95×10^{-4}, 3.71×10^{-4}, 3.97×10^{-4} and 8.31×10^{-4} cm/s while the MW is increased from 6.3 to 33.6 kg/mol. Thus, the Si-PCPDTTBT with higher MW results not only a larger mobility but also a decreased value of R_{ct}, that leads to a larger value of k_0.

The ΔOD as a function of charge ingress/egress are shown in Fig. 7 at a monochromatic wavelength of 550 nm. The relationship was determined by switching voltages between a fixed darkened state (−0.1 V) and different bleached states. By calculating the slope of ΔOD vs. charge plot, the CEs of Si-PCPDTTBT can be determined. The calculated CE of 33.6 kg/mol Si-PCPDTTBT is 423 cm^2/C, which is much higher than that of 6.3 kg/mol one (226 cm^2/C). As described above, the crystalline structure of the high MW Si-PCPDTTBT is responsible for its larger charge mobility and lower value of *R*ct at the polymer film-electrolyte interface. These properties can minimize the inject/eject charge. Moreover, the ΔOD also increases with increasing MWs as shown in Fig. 3. These factors both enhance the CE for higher MW Si-PCPDTTBT.

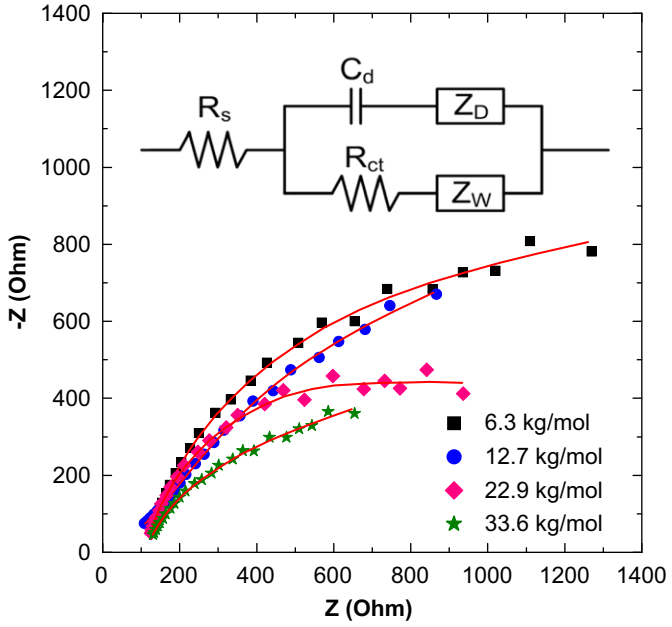

Fig. 6. EIS results of Si-PCPDTTBT films with various MWs.

For electrochromic switching studies, polymer films were coated on ITO-coated glass slides in the same manner as described above. The transmittance in response to the potential was repeatedly switched between 0 and 1.0 V (10 s for each). The 33.6 kg/mol Si-PCPDTTBT delivers a Δ%*T* of 48% at 580 nm. As depicted in Fig. 8, the Si-PCPDTTBT thin film reveals a switching time of 2.2 s at 1.0 V for the bleached process and 2.4 s for the darkened process. The ratio of the bleached and the darkened switching time is 91.7%, indicating that charge injection/ejection was reversible during electrochemical reactions.

In addition to the optical spectra, we also performed colorimetry analysis, which provided a more precise way than optical spectra to define color. The CIE 1931 color space coordinates of the Si-PCPDTTBT with the applied voltage of 0 V and 1.0 V are determined to be (0.2521, 0.1121) and (0.2491, 0.2687), respectively. The polymer switched from deep purple neutral state at 0 V to pale-blue oxidized state at 1.0 V are shown in the inset of Fig. 9. The luminance dependence on the applied potential for Si-PCPDTTBT is also shown in the inset of Fig. 9. As expected for a cathodically coloring material, the luminance increases upon

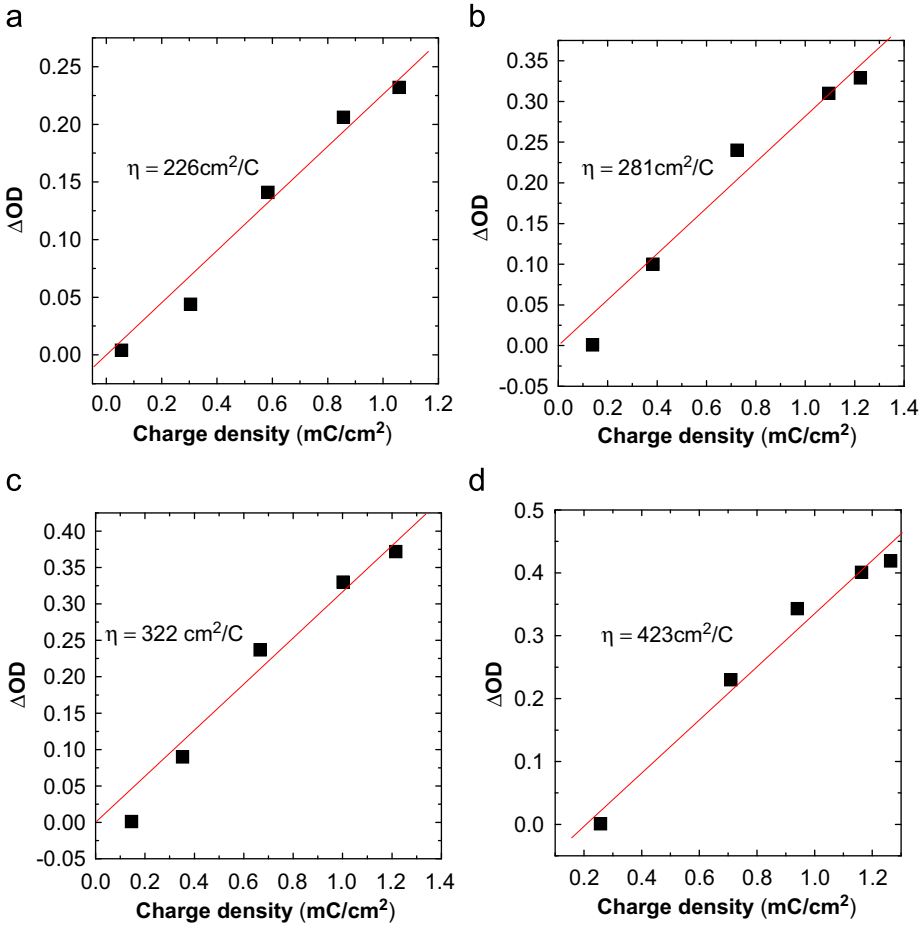

Fig. 7. Optical density changes of Si-PCPDTTBT thin films as a function of intercalated charge density.

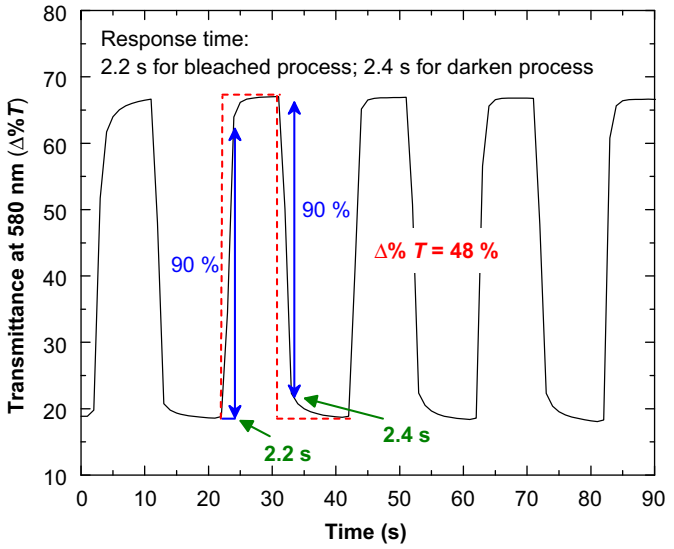

Fig. 8. Optical transmittance changes for the 33.6 kg/mol Si-PCPDTTBT at 580 nm, stepped between 0.0 and 1.0 V (vs. Ag/Ag^+).

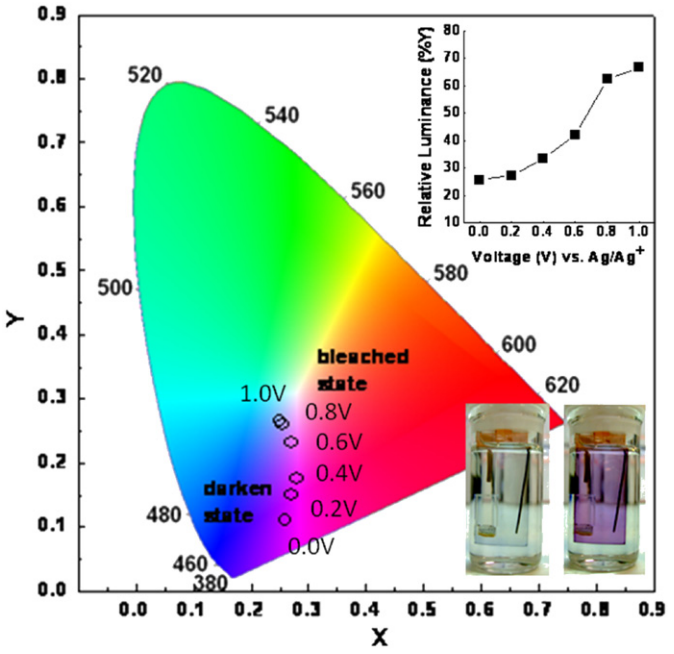

Fig. 9. CIE 1931 *xy* chromaticity diagram for the 33.6 kg/mol Si-PCPDTTBT and the relative luminance (%*Y*) at applied potentials ranging from 0 to 1.0 V (vs. Ag/Ag^+). The images are the Si-PCPDTTBT film under darken and bleached states. (For interpretation of the references to color in this figure legend, the reader is referred to the web version of this article.)

oxidation from 25.6% to 66.7%, as the intensity of the π–π^* transition diminishes.

4. Conclusion

We conclude that the MW of Si-PCPDTTBT has a substantial effect on the way that the polymer chains stacked on each other. This characteristic affects the charge mobility by three times as we increase the Si-PCPDTTBT MW from 6.3 to 33.6 kg/mole. Moreover, the ΔOD of Si-PCPDTTBT also increases with increasing MW. Combining the two factors, the electrochromic CE can be enhanced from 226 to 423 cm^2/C when the MW of polymers is increased from 6.3 to 33.6 kg/mol.

Acknowledgments

The authors are grateful to the National Science Council (NSC), Taiwan (NSC 98-2221-E-001–002 and 99-2120-M-009-008) and Academia Sinica for financial support.

References

[1] S. Koyuncu, O. Usluer, M. Can, S. Demic, S. Icli, N.S. Sariciftci, Electrochromic and electroluminescent devices based on a novel branched quasi-dendric fluorene-carbazole-2,5-bis(2-thienyl)-1H-pyrrole system, Journal of Materials Chemistry 21 (2011) 2684–2693.
[2] C.M. Amb, A.L. Dyer, J.R. Reynolds, Navigating the color palette of solution-processable electrochromic polymers, Chemistry of Materials 23 (2011) 397–415.
[3] G. Hızalan, A. Balan, D. Barana, L. Toppare, Spray processable ambipolar benzotriazole bearing electrochromic polymers with multi-colored and transmissive states, Journal of Materials Chemistry 21 (2011) 1804–1809.
[4] M.A. Invernale, Y. Ding, G.A. Sotzing, All-organic electrochromic spandex, ACS Applied Materials and Interfaces 2 (2010) 296–300.
[5] J.H. Huang, C.Y. Hsu, C.W. Hu, C.W. Chu, K.C. Ho, The influence of charge trapping on the electrochromic performance of poly(3,4-alkylenedioxythiophene) derivatives, ACS Applied Materials and Interfaces 2 (2010) 351–359.
[6] J. Ding, M. de Miguel, J. Lu, Y. Tao, H. García, Rapid switching and high contrast electrochromic property by electrochemical reduction of an alternating copolymer of fluorene and oxadiazole, Journal of Physical Chemistry C 114 (2010) 5168–5173.
[7] S. Bhandari, M. Deepa, A.K.S. Srivastava, C. Lal, R. Kant, Poly(3,4-ethylenedioxythiophene) (PEDOT)-coated MWCNTs tethered to conducting substrates: facile electrochemistry and enhanced coloring efficiency, Macromolecular Rapid Communications 29 (2008) 1959–1964.
[8] S. Bhandari, M. Deepa, S.N. Sharma, A.G. Joshi, A.K. Srivastava, R. Kant, Charge transport and electrochromism in novel nanocomposite films of poly(3,4-ethylenedioxythiophene)-Au nanoparticles–CdSe quantum dots, Journal of Physical Chemistry C 114 (2010) 14606–14613.
[9] S. Bhandari, M. Deepa, A.K. Srivastava, A.G. Joshi, R. Kant, Poly(3,4-ethylenedioxythiophene)–multiwalled carbon nanotube composite films: structure-directed amplified electrochromic response and improved redox activity, Journal of Physical Chemistry B 113 (2009) 9416–9428.
[10] S. Xiong, J. Wei, P. Jia, L. Yang, J. Ma, X. Lu, Water-processable polyaniline with covalently bonded single-walled carbon nanotubes: enhanced electrochromic properties and impedance analysis, ACS Applied Materials and Interfaces 3 (2011) 782–788.
[11] J.H. Huang, C.Y. Yang, C.Y. Hsu, C.L. Chen, L.Y. Lin, R.R. Wang, K.C. Ho, C.W. Chu, Solvent-annealing-induced self-organization of poly(3-hexylthiophene), a high-performance electrochromic material, ACS Applied Materials and Interfaces 1 (2010) 2821–2828.
[12] V. Jain, R. Sahoo, S.P. Mishra, J. Sinha, R. Montazami, H.M. Yochum, J.R. Heflin, A. Kumar, Synthesis and characterization of regioregular water-soluble 3,4-propylenedioxythiophene derivative and its application in the fabrication of high-contrast solid-state electrochromic devices, Macromolecules 42 (2009) 135–140.
[13] R.J. Kline, M.D. McGehee, E.N. Kadnikova, J. Liu, J.M.J. Fréchet, Controlling the field-effect mobility of regioregular polythiophene by changing the molecular weight, Advanced Materials 15 (2003) 1519–1522.
[14] R.C. Hiorns, R. de Bettignies, J. Leroy, S. Bailly, M. Firon, C. Sentein, A. Khoukh, H. Preud'homme, C. Dagron-Lartigau, High molecular weights, polydispersities, and annealing temperatures in the optimization of bulk-heterojunction photovoltaic cells based on poly(3-hexylthiophene) or poly(3-butylthiophene), Advanced Functional Materials 16 (2006) 2263–2273.
[15] L.M. Andersson, Charge transport and energetic disorder in polymer:fullerene blends, Organic Electronics 12 (2011) 300–305.
[16] D.J.D. Moet, M. Lenes, J.D. Kotlarski, S.C. Veenstra, J. Sweelssen, M.M. Koetse, B. de Boer, P.W.M. Blom, Impact of molecular weight on charge carrier dissociation in solar cells from a polyfluorene derivative, Organic Electronics 10 (2009) 1275–1281.
[17] K. Hosoi, T. Mori, T. Mizutani, T. Yamamoto, N. Kitamura, Effects of molecular weight on polyfluorene-based polymeric light emitting diodes, Thin Solid Films 438–439 (2003) 201–205.
[18] C.G. Wu, M.I. Lu, P.F. Tsai, Full-color processible electrochromic polymers based on 4,4-dioctyl-cyclopentadithiophene, Macromolecular Chemistry and Physics 210 (2009) 1851–1855.
[19] H.C. Ko, J. Yom, B. Moon, H. Lee, Electrochemistry and electrochromism of a poly(cyclopentadithiophene) derivative with a viologen pendant, Electrochimica Acta 48 (2003) 4127–4135.

[20] J.H. Huang, C.M. Teng, Y.S. Hsiao, F.W. Yen, P. Chen, F.C. Chang, C.W. Chu, Nanoscale correlation between exciton dissociation and carrier transport in silole-containing cyclopentadithiophene-based bulk heterojunction films, Journal of Physical Chemistry C115 (2011) 2398–2405.
[21] J.H. Huang, F.C. Chen, C.L. Chen, A.T. Huang, Y.S. Hsiao, C.M. Teng, F.W. Yen, P. Chen, C.W. Chu, Molecular-weight-dependent nanoscale morphology in silole-containing cyclopentadithiophene polymer and fullerene derivative blends, Organic Electronics 12 (2011) 1755–1762.
[22] F. Sundfors, J. Bobacka, A. Ivaska, A. Lewenstam, Kinetics of electron transfer between $Fe(CN)_6^{3-/4-}$ and poly(3,4-ethylenedioxythiophene) studied by electrochemical impedance spectroscopy, Electrochimica Acta 47 (2002) 2245–2251.
[23] T.A. Skotheim, J.R. Reynolds (Eds.), Handbook of Conducting Polymers, third ed., CRC Press, Boca Raton, FL, vol. 2, Chapter 20, 2007.
[24] J.H. Huang, C.Y. Yang, Z.Y. Ho, D. Kekuda, M.C. Wu, F.C. Chien, P. Chen, C.W. Chu, K.C. Ho, Annealing effect of polymer bulk heterojunction solar cells based on polyfluorene and fullerene blend, Organic Electronics 10 (2009) 27–33.
[25] M. Shin, H. Kim, S. Nam, J. Park, Y. Kim, Influence of hole-transporting material addition on the performance of polymer solar cells, Energy and Environmental Science 3 (2010) 1538–1543.
[26] Y. Zhou, M. Eck, M. Krüger, Bulk-heterojunction hybrid solar cells based on colloidal nanocrystals and conjugated polymers, Energy and Environmental Science 3 (2010) 1851–1864.
[27] M.K. Siddiki, J. Li, D. Galipeau, Q. Qiao, A review of polymer multijunction solar cells, Energy and Environmental Science 3 (2010) 867–883.
[28] M. Brinkmann, J.C. Wittmann, Orientation of regioregular poly(3-hexylthiophene) by directional solidification: a simple method to reveal the semicrystalline structure of a conjugated polymer, Advanced Materials 18 (2006) 860–863.
[29] C. Melzer, E.J. Koop, V.D. Mihailetchi, P.W.M. Blom, Hole transport in poly(phenylene vinylene)/methanofullerene bulk-heterojunction solar cells, Advanced Functional Materials 14 (2004) 865–870.